

# Proposed Formulas for Estimating Splitting Tensile, Shear and Flexural Strengths, and Long Term Deflection Assessment of Self-Compacting Concrete Elements

Mohammed S. Al-Ansari<sup>1</sup>, Ala G. Abu Taqa<sup>1,\*</sup>, Ahmed B. Senouci<sup>2</sup>, Neil N. Eldin<sup>2</sup>, Mohamed Helal<sup>3</sup>, and Cesar Asiado<sup>3</sup>

<sup>1</sup>Department of Civil and Architectural Engineering, Qatar University, P.O. Box 2713, Doha, Qatar

<sup>2</sup>Department of Construction Management, University of Houston, Houston, TX 77204-4020, Texas, USA

<sup>3</sup>Al Wataniya Concrete Company, P.O. Box: 24381, Doha, Qatar

## ABSTRACT

This paper investigated the splitting tensile and shear strengths and the modulus of rupture of Self Compacting Concrete (SCC) elements with fly ash, micro silica and polycarboxylate ether superplasticizer for various grades and water-to-binder ratios. The immediate and long term deflections of SCC beams were also studied. Finally, the experimental values of the mechanical properties of SCC elements were compared to those computed using ACI-318 design code equations that were formulated for Normally Vibrated Concrete (NVC). The novelty of this study lies in the proposal of alternatives to ACI-318 design code formulas to account for the use of SCC in place of NVC. Moreover, the paper provides an assessment of the long term deflection of SCC beams.

**KEYWORDS:** Self Compacting Concrete, Splitting Tensile Strength, Shear Strength, Flexural Strength, Modulus of Rupture, Long Term Deflection.

## 1. INTRODUCTION

Self-Compacting Concrete (SCC), also known as Self-Consolidating Concrete, is an innovative concrete that does not need vibration or compaction. Due to its high workability, SCC can easily flow under its own weight to achieve full compaction. Hence, SCC may be the best viable solution in the presence of congested reinforcement. High performance SCC mixes exhibit these attractive benefits while maintaining the mechanical and durability characteristics of NVC.

The materials used in SCC are the same as those used for NVC. However, a portion of the cement is replaced with fine powdered materials (i.e., fly ash, silica fume, limestone powder, glass filler, and quartzite filler) and chemical admixtures are used to reduce air voids within the concrete mixture. A viscosity modifying agent (VMA) may be also required to avoid the segregation and instability of the mix, which may occur due to the variations in the proportions of water, aggregate and sand.

Because of the current high rate of economic growth and urban development, huge investments are directed towards infrastructure projects such as airports, metro systems, high-speed rail networks, residential towers, and hotels. The construction of these infrastructure projects requires new construction techniques and materials that can save time and cost. SCC is a promising material for the construction industry because it generates substantial time and cost savings.

SCC has experienced limited civil engineering applications in several countries since its development.<sup>2–7</sup> However, its use in construction applications has experienced a steady and gradual increase in the last few years. For example, SCC jacketing was successfully applied to rehabilitate deficient or damaged RC beam.<sup>8–12</sup> Hence, an extensive knowledge on fresh and hardened properties of SCC is becoming increasingly critical.

Significant research was conducted on the mix design and rheological properties of SCC.<sup>13–15</sup> Moreover, researchers have recently created databases to develop an overall view of the mechanical aspects of SCC. For example, Holschemacher and Klug<sup>16</sup> created a database using SCC published experimental results on compressive and tensile strengths, elastic modulus, and bond properties.

\*Author to whom correspondence should be addressed.

Email: [ala.abutaqa@qu.edu.qa](mailto:ala.abutaqa@qu.edu.qa)

Received: 30 January 2017

Accepted: 24 May 2017

They concluded that the design rules of NVC are still applicable to SCC. Domone<sup>17</sup> analyzed SCC hardened properties data that was collected from more than 70 studies. He also correlated the collected data to compare the hardened properties of SCC to those of NVC. Craeye et al.<sup>18</sup> studied whether the existing design codes formulae, which are originally proposed for NVC are still valid to be used for SCC. They have constructed a comprehensive database from more than 250 research papers that were published on the fresh and hardened properties of SCC between 1990 and 2011. The results of the elastic modulus and tensile strength (direct, splitting, and flexure) were studied and compared to those computed using the design code equations developed for NVC (e.g., Eurocode 2 (EC2) and Model code (MC90 or MC2010)). Moreover, the effects of the mix design parameters such as aggregate type, paste volume, water-to-cement ratio (W/C), water-to-binder ratio...etc. on the elastic modulus and tensile strength of SCC were investigated. Golafshani and Ashour<sup>19</sup> introduced one of the most recent studies on the prediction of the elastic modulus of SCC using a novel symbolic regression approach namely biogeographical-based programming (BBP). Their model was constructed directly from a comprehensive dataset of experimental results of SCC available in the literature. Another new symbolic regression model, namely artificial bee colony programming (ABCP), were also developed for comparison purposes. The results of both model were then compared to those computed using various design code equations including ACI-318 code.<sup>1</sup> They reported that ACI-318 code provides reasonable prediction of the SCC elastic modulus. This contradicts the findings of Craeye et al.<sup>18</sup> who reported that ACI-318 code<sup>1</sup> underestimates the absolute value of the SCC elastic modulus.

The splitting tensile and shear strengths of concrete are important parameters used in the design of reinforced concrete structures. The splitting tensile strength is used for computing the development length of the reinforcing steel bars while the shear strength is needed for the shear design of reinforced concrete elements. The database provided by Craeye et al.<sup>18</sup> showed that the paste volume, filler type, and coarse aggregate size do not affect the splitting tensile strength of SCC while the aggregate type does. Parra et al.<sup>20</sup> studied the splitting tensile strength and the elastic modulus for SCC of different ages and compared them to those of NVC. They reported that the splitting tensile strength of SCC was on average 15% less than that of NVC. They have recommended that the design equations used for NVC be modified for SCC but they did not provide any modifications. This agrees with the findings of Filho et al.<sup>21</sup> who reported that the compressive strength and splitting tensile strength of SCC are lower than those computed using most design code equations. However, Domone<sup>17</sup> and Craeye et al.<sup>18</sup> reported the validity of the SCC splitting tensile strengths computed using Eurocode (EC2) and Model 2010 (MC2010) design equations.

Kim et al.<sup>22</sup> studied the influence of the aggregate and paste volumes on the shear capacity of SCC specimens for various coarse aggregate types, volumes, and compressive strengths. They proposed new equations for the determination of the concrete shear strength for SCC mixtures. Moreover, Boel et al.<sup>23</sup> examined the shear capacity of SCC and compared them to those obtained for NVC. The results showed a slight decrease of shear capacity for SCC compared to NVC for a given compressive strength. According to their study, the shear capacity decreased with increasing shear span-to-depth ratio for all tested concrete types.

The long-term behavior of SCC is also important for the deflection computation of structural elements. Mazzotti and Savoia<sup>24</sup> investigated the long-term behavior of reinforced SCC beams. They reported that the long-term behavior of SCC is qualitatively similar to that of NVC in terms of total shrinkage and total creep. However, they reported that the creep and shrinkage of SCC were larger than those of NVC. The authors also mentioned that the long-term deflection rate of beams under flexure was almost constant, in log time scale, after the same period of time. Moreover, it was found that SCC crack widths increased only slightly under the long term loading. Hence, their contribution to the long-term deflection could be neglected.

ACI Committee 237<sup>25</sup> reported the current state of the knowledge and provided target guidelines for fresh and hardened properties of SCC. It also specified the testing methods and guidelines for the transportation, placement, and selection of SCC proportions. On the other hand, ACI-318 building design code<sup>1</sup> provided formulae for predicting the mechanical properties of normal and light weight concrete elements. However, it does not provide provisions for estimating the mechanical properties of SCC elements.

## 2. RESEARCH SIGNIFICANCE

In this paper, the splitting tensile strength, shear strength, modulus of rupture, and long term deflection of SCC mixes containing fly ash and micro silica were studied for various grades (i.e., 40 MPa, 50 MPa and 60 MPa) and various Water-to-Binder ratios W/B (i.e., 0.35 and 0.45). The SCC mechanical properties results were then compared to those predicted using ACI-318 code equations. The behavior of SCC and NVC elements may differ. Therefore, it is important to determine whether the ACI design code equations that were developed for NVC elements are still applicable for SCC elements. This study compares the mechanical properties of SCC elements obtained experimentally to those computed using the ACI code equations. It does not compare between the behavior of SCC and NVC elements as widely reported in literature. This study is novel and proposes for the first time alternative formulas for estimating the mechanical properties of concrete elements when SCC is used instead of NVC. The SCC mixes investigated

in this study contained fly ash and micro silica as filler materials. However, more experimental research need to be directed towards other SCC mixes with different filler material types to develop general formulae for estimating the mechanical properties of SCC elements.

### 3. EXPERIMENTAL SECTION

Three tests were carried out on SCC specimens, namely, splitting tensile and shear strengths, and modulus of rupture (i.e., flexural strength). The specimens were casted and cured according ASTM C192.<sup>26</sup> The long term deflection of SCC beams was investigated for a period of one year.

#### 3.1. Materials

All SCC mixes were prepared using Ordinary Portland Cement (OPC), 4–10 mm and 10–20 mm diameter coarse aggregates, natural sand (0–4 mm diameter), 25% fly ash, 5% micro silica and Polycarboxylate Ether Superplasticizer (Epsilone HP 540) with a proportion of 1.4 to 1.6% by cement weight to achieve the required slump of SCC mixes. As reported by Harkouss and Hamad,<sup>27</sup> the optimum superplasticizer dosage to produce a high workable SCC mix (with 60 MPa compressive strength and about 0.34 W/C ratio) may be taken as 1.6% by weight of cement. The superplasticizer dosage is taken herein between 1.4% and 1.6% by weight of cement according to the concrete grade and W/C of the mix. Table I summarizes SCC materials along with their sources, suppliers, and types.

#### 3.2. Mixture Composition

To cover the usual range of compressive strengths used in building construction, six different self-compacting concrete mixes were designed by the ready mix company using three different concrete grades (i.e., 40 MPa, 50 MPa and 60 MPa) and two different water-to-binder ratios

(i.e., 0.35 and 0.45). The selection of the mixture composition was based on ACI 237R.<sup>25</sup> The binder consisted of cement, fly ash and micro silica. The concrete mix designs and proportions are summarized in Table II.

#### 3.3. Fresh Concrete Properties

The fresh concrete properties for all mixes, namely, temperature (ASTM C1064<sup>28</sup>), slump flow (BS EN 12350-8<sup>29</sup>), and V-funnel tests (BS EN 12350-9<sup>30</sup>), were checked immediately after mixing and 1 hour after that. The obtained results, which are summarized in Table III, were found to be within the SCC mix acceptable limits that were specified by ACI committee 237 report<sup>25</sup> and the European guidelines for self-compacting concrete.<sup>31</sup>

#### 3.4. Hardened Concrete Properties

##### 3.4.1. Splitting Tensile Strength Test

The tested specimens were standard cylinders according to ASTM C470<sup>32</sup> (i.e., 152 mm in diameter and 304 mm in length). Twelve specimens were made from each mix. Six specimens were tested in compression and six in splitting tension. The compression and splitting tension tests of the specimens were done after 28 days of moist curing according to ASTM C39<sup>33</sup> and ASTM C496,<sup>34</sup> respectively.

##### 3.4.2. Modulus of Rupture (Flexure Strength) Test

The tested specimens were plain concrete beams with the following dimensions: (1) 100 mm × 100 mm × 500 mm and (2) 150 mm × 150 mm × 750 mm. Four beams from each size were prepared from each mix in addition to four standard cylinders to be tested under compression. The compression and flexural strength tests of specimens were carried out after 28 days of moist curing according to ASTM C39<sup>33</sup> and ASTM C78,<sup>35</sup> respectively.

##### 3.4.3. Shear Strength Test

Two beam specimens were used for the shear strength test. The first one had dimensions of 100 mm × 100 mm × 500 mm and was reinforced with 2T10 bottom Grade 60 reinforcing steel bars ( $f_y = 420$  MPa) satisfying ASTM A615M.<sup>36</sup> On the other hand, the second beam specimen had the dimensions of 150 mm × 150 mm × 750 mm and was reinforced with 3T10 bottom reinforcing steel bars. To ensure that the specimens fail under shear, no stirrups were provided in the beams.

Four beams from each size were prepared from each mix along with four standard cylinders to be tested in compression. The compression strength test was conducted according to ASTM C39.<sup>33</sup> On the other hand, the shear strength test was carried out using a four-point loading scheme as shown in Figure 1, with two different shear span to depth ratios ( $a/d$ ). Two beams from each size were tested with ( $a/d$ ) = 1.5 and the other two beams of same size were tested with ( $a/d$ ) = 2.0. Figure 2 shows a typical beam shear failure.

**Table I.** SCC mixture components.

Material	Source	Type/conformity
Cement	Qatar	OPC class 42.5N, Conformance to EN 197-1
Fly ash	India	CLASS F, conformance to ASTM C 618
Micro silica	Qatar	Conformance to ASTM C 1240
Coarse aggregate 20 mm and 10 mm	UAE	Crushed gabbro, conformance to BS EN 12620
Fine aggregate (washed sand)	Qatar	Natural, conformance to BS EN 12620
Epsilone HP 540	Qatar	Polycarboxylate ether superplasticizer, conformance to BS EN 934-2 and ASTM C 494 type D and G, specific gravity @ 25 °C = 1.075 ± 0.02, chloride content: NIL

**Table II.** SCC mix designs and proportions.

Constituent material (kg/m <sup>3</sup> )	SCC40/0.35	SCC40/0.45	SCC50/0.35	SCC50/0.45	SCC60/0.35	SCC60/0.45
Cement	301	280	308	294	315	301
Fly ash	107.5	100	110	105	112.5	107.5
Micro silica	21.5	20	22	21	22.5	21.5
Coarse aggregate 20 mm	392	382	427	409	403	386
Coarse aggregate 10 mm	490	477	485	465	423	533
Fine aggregate (washed sand)	967	941	922	884	878	824
Water	151	180	154	189	158	194
Epsilone HP 540	4.5	4.5	5	4.5	4.5	4.5

### 3.4.4. Long Term Deflection Test

Because of the relatively high cost of the test, only two concrete mixes were used for the long term deflection, namely SCC 40/0.45 (i.e., concrete grade of 40 MPa and W/B ratio of 0.45) and SCC 60/0.35 (refer to Table II).

8 beams with a cross section of 200 mm × 250 mm and a length of 2500 mm were prepared. The beams were divided into 2 groups of four based on their concrete grade. Each beam was reinforced with 2T20 Grade 60 bottom reinforcing steel bars satisfying ASTM A615M.<sup>36</sup> This is equivalent to a steel ratio of 0.015, which is below the balanced value for all cases but in the practical range. The top (compression) reinforcement was different for each beam group. Two beams were reinforced with a top reinforcement equal to 65% of the bottom steel, which was provided by 2T16 reinforcing steel bars. The other two beams were reinforced with top reinforcement equal to the bottom steel (i.e., 2T20). A shear reinforcement of T10@100 mm was also provided. Figure 3 shows the beam steel reinforcement detailing.

The beams were prepared on site and demolded after 24 hours. They were then moist cured for 6 days and air cured on site from the 7th to 28th day. To determine the failure load, four beams, two from each group were tested up to failure using four points loading scheme on the 28th day after casting as shown in Figure 4. Figure 5 shows beam cracking and failure. In order to minimize self-weight creep deflections, the other four beams were not moved from their casting position.

After being transferred to the university lab, the beams were placed on specially designed steel supports.

A superimposed dead load of concrete blocks was then hung from the beams using steel plates and bolts at four points to simulate a uniform load as shown in Figure 6. The weight of each block is equal to 1 ton ( $\approx 10$  kN). This loading configuration represents about 20% of the average failure load. As soon as the beams were fully loaded, the initial deflections due to the superimposed load were recorded using strain gauges fixed at mid span. The time dependent deformations were recorded at the 7th and 14th day and every month after that for a period of 6 months.

## 4. RESULTS AND DISCUSSION

It is worth noting that the outlying observations were first checked for all the tests to identify the samples that deviate significantly from the rest. This is an important check during the analysis of the test results because the underlying observations may result from several sources such as recording errors, numerical calculation errors, and equipment errors.

According to ASTM E178<sup>37</sup> criterion, the test statistic for measured outliers is the difference between the test values and their average divided by the standard deviation. The test statistic values should be compared to the critical value shown in ASTM E178-08<sup>37</sup> Table I for the two-sided test at the 1.0% significance level or for the one-sided test at the 0.50% significance level. This decision is conform to the ASTM E178<sup>37</sup> recommendation that a low significance level, such as 1.00% is to be used as the critical value to test outlying observations. To be considered as an outlier, the observation test criterion should exceed

**Table III.** Fresh concrete properties.

Test	SCC40/0.35	SCC40/0.45	SCC50/0.35	SCC50/0.45	SCC60/0.35	SCC60/0.45
Temperature (°C)						
Immediate	24.6	25.2	24.0	24.3	24.8	24.6
1 Hour	24.1	24.9	23.4	23.9	24.0	24.1
Slump flow (mm) (550 mm–850 mm)						
Immediate	750	765	725	755	655	670
1 Hour	710	725	655	675	600	640
V-Funnel (sec.) (<25 sec.)						
Immediate	5.5	5.37	4.57	5.09	5.5	5.0
1 Hour	4.5	4.11	5.99	5.57	5.4	5.2



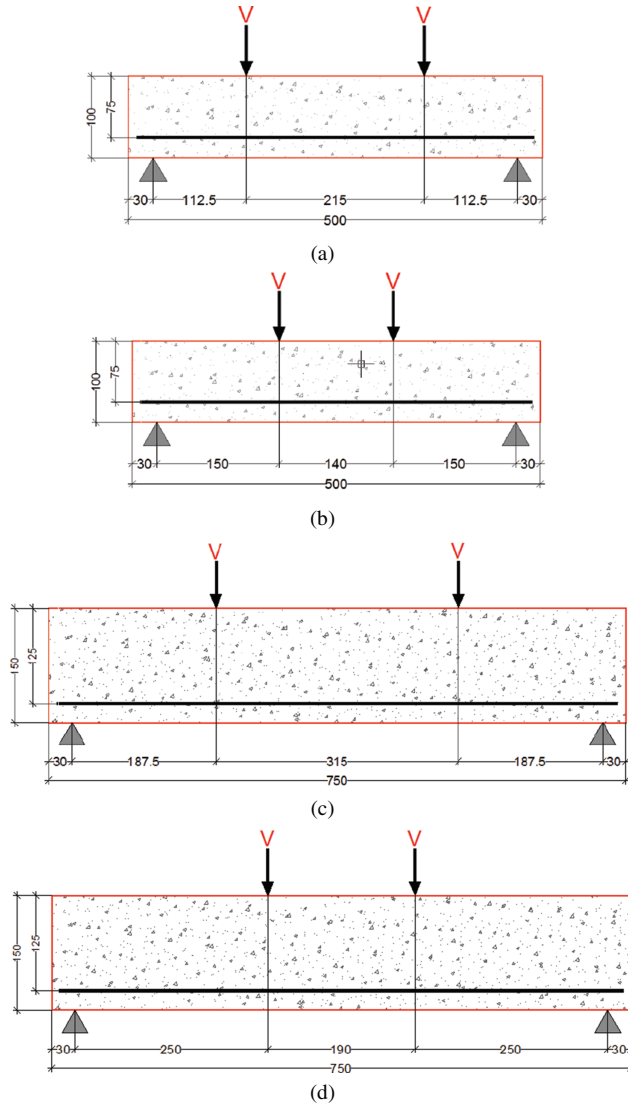


**Fig. 1.** Four point loading scheme for shear strength test: (a)  $100 \times 100 \times 500$  mm beams with  $a/d = 1.5$ ; (b)  $100 \times 100 \times 500$  mm beams with  $a/d = 2$ ; (c)  $150 \times 150 \times 750$  mm beams with  $a/d = 1.5$ ; (d)  $150 \times 150 \times 750$  mm beams with  $a/d = 2$ .

the critical value. Table I of ASTM E178-08<sup>37</sup> shows that the critical values for one-sided test corresponding to 4 and 6 repetitions with 0.50% significance level are 1.496 and 1.937, respectively. Hence, all samples that satisfy the



**Fig. 2.** Beam shear failure.

following condition were considered herein as outliers

$$\frac{x_i - \bar{x}}{\sigma} \geq \begin{cases} 1.496 \text{ for 4 samples} \\ 1.937 \text{ for 6 samples} \end{cases} \quad (1)$$

Where  $x_i$  = test value,  $\bar{x}$  = average test value, and  $\sigma$  = standard deviation.

After eliminating the outlier results, the average of the remaining samples could be considered.

#### 4.1. Splitting Tensile Strength Test

The compressive strength was calculated using the following formula (ASTM C39):

$$f'_c = \frac{4P}{\pi d^2} \quad (2)$$

Where,  $f'_c$  = compressive strength, MPa;  $P$  = maximum applied load, N; and  $d$  = specimen diameter, mm.

According to ASTM C496, the splitting tensile strength was calculated using the following formula:

$$f_{ct} = \frac{2P}{\pi dL} \quad (3)$$

Where,  $f_{ct}$  = splitting tensile strength, MPa and  $L$  = specimen length, mm.

The loading rate used for compression and splitting tensile tests were 0.25 MPa/s and 0.018 MPa/s, respectively. This conforms to the requirements of ASTM C39<sup>33</sup> and ASTM C496<sup>34</sup> standards. Table IV summarizes the averages of the compressive and splitting tensile test results for all mixes.

Table IV shows that the average ratio of the experimental splitting tensile strength and the square root of the compressive strengths is around 0.50. This ratio decreases as the water/cement ratio increases because of the drop in both strengths. Knowing that the ratio specified by the ACI code for NVC is equal to 0.57, the ratio of  $f_{ct}(\text{SCC})$  to  $f_{ct}(\text{ACI-318})$  is given by the following equation:

$$\frac{f_{ct(\text{SCC})}}{f_{ct(\text{ACI-318})}} = \frac{0.50\sqrt{f'_c}}{0.57\sqrt{f'_c}} = 0.878 \quad (4)$$

This ratio is with a good agreement with the findings of Parra et al.<sup>20</sup> who reported a value of 0.845.

In order to compare the splitting tensile strength results obtained in this study to those obtained using the ACI-318 design code<sup>1</sup> equation, the relationship between the experimental average splitting tensile strengths and the square root of the average compressive strengths was plotted as shown in Figure 7. The linear regression equation of the experimental data was also determined and compared to the ACI-318 code<sup>1</sup> design formula.

Figure 7 shows that the splitting tensile strength values of SCC are lower than those computed using ACI-318<sup>1</sup> formula for NVC. The splitting tensile strength of SCC

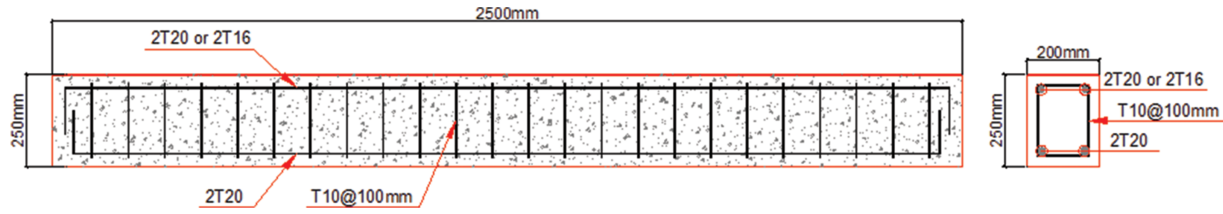


Fig. 3. Beam dimensions and reinforcement for long term deflection test.

can alternatively be computed using the following linear regression equation:

$$f_{cr(scc)} = 0.739\sqrt{f'_c} - 1.753 \quad (5)$$

However, more research work needs to be conducted in order to propose reliable modifications to ACI-318<sup>1</sup> formula to accurately model the splitting tensile behavior of SCC.

#### 4.2. Modulus of Rupture (Flexure Strength) Test

The compressive strength of the cylindrical specimens was calculated using Eq. (2). It is worth noting that the fracture of all tested beams started in the tension surface within the middle third of the span length. Hence, the modulus of rupture can be calculated using the following formula (ASTM C78<sup>35</sup>):

$$f_r = \frac{PL}{bd^2} \quad (6)$$

Where,  $f_r$  = modulus of rupture, MPa;  $P$  = maximum applied load, N;  $L$  = specimen length, mm;  $b$  = specimen average width, mm and  $d$  = specimen diameter, mm.

Table V summarizes the average compressive and modulus of rupture values for all mixes. It shows that the average ratio between the modulus of rupture and the square root of the compressive strength is around 0.71. This ratio also decreases as the water/cement ratio increases. It is worth noting that the ratio specified by the ACI code for NVC is equal to 0.62. Therefore, ACI-318<sup>1</sup> equation related to modulus of rupture of NVC may be conservatively used for SCC without modification.

In order to compare the modulus of rupture results obtained in this study to those obtained using the ACI-318 design code<sup>1</sup> equation, the relationship between the experimental average modulus of rupture and the square root of the average compressive strength was plotted as shown

in Figure 8. The figure shows that the modulus of rupture values of SCC are higher than those computed using ACI-318 formula for NVC. The modulus of rupture of SCC can alternatively be computed using the following linear regression equation:

$$f_{r(scc)} = 1.665\sqrt{f'_c} - 6.438 \quad (7)$$

However, more research work needs to be conducted in order to be propose reliable modifications to ACI-318<sup>1</sup> formula to accurately model the splitting tensile behavior of SCC.

#### 4.3. Shear Strength Test

The compressive strength of the cylindrical specimens was calculated using the Eq. (2). The shear strength of the tested beams was calculated using the following equation:

$$v = \frac{P}{bd} \quad (8)$$

Where,  $v$  = shear strength, MPa;  $P$  = maximum applied load, N;  $b$  = specimen average width, mm and  $d$  = specimen diameter, mm.

Table VI shows the ratios between the NVC shear strength computed using ACI-318 code<sup>1</sup> equation and the experimental SCC shear strength values for two shear span to depth ratios. As per ACI-318 code<sup>1</sup> Section 22.5.5.1, the shear strength of NVC is equal to the smallest value of the following expressions:

$$v = \left\{ \begin{array}{l} 0.16\sqrt{f'_c} + 17\rho \frac{V_u d}{M_u} \\ 0.16\sqrt{f'_c} + 17\rho \\ 0.29\sqrt{f'_c} \end{array} \right\} \quad (9)$$

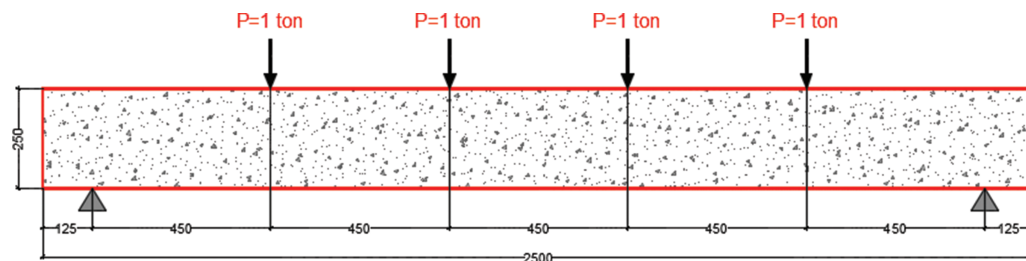
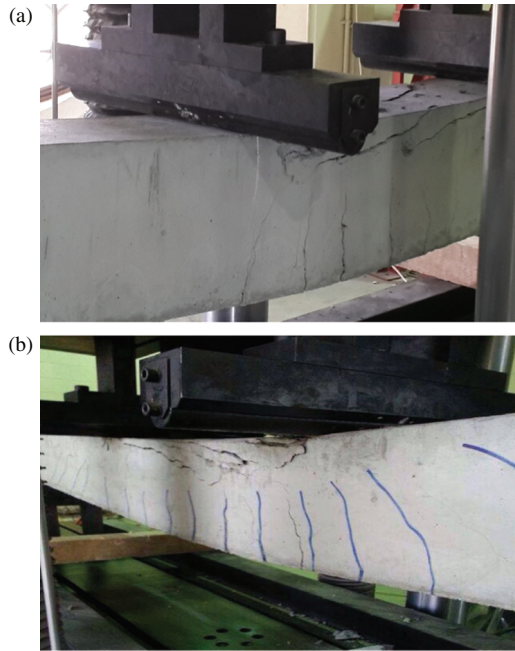


Fig. 4. Four point loading scheme for long term deflection test (dimensions are in mm).



**Fig. 5.** Long term deflection test: (a) Beam cracking; (b) beam failure.

However, for design purposes, ACI-318 code assumes the second term in the first two expressions equals to  $0.01\sqrt{f'_c}$ . Accordingly, the code suggests using Eq. (10) to calculate the shear capacity regardless the values of the shear span or section depth:

$$v = 0.17\sqrt{f'_c} \quad (10)$$

Table VI shows that the experimental shear values obtained for a shear span to depth ratio of 1.5 were higher than those obtained for a shear span to depth ratio of 2.0, indicating similar shear behavior of NVC (Kani's valley).<sup>38</sup>

Figure 9 shows the relationship between the shear strength for shear span to the depth ratios of 1.5 and 2.0 and the square root of the compressive strength. It also shows the relationship between the shear strength  $f_{ct}$  computed using general ACI-318 code<sup>1</sup> equation and the square root of the compressive strength.

The best fit linear regression model of the experimental data for both shear to span ratios shown in Figure 9

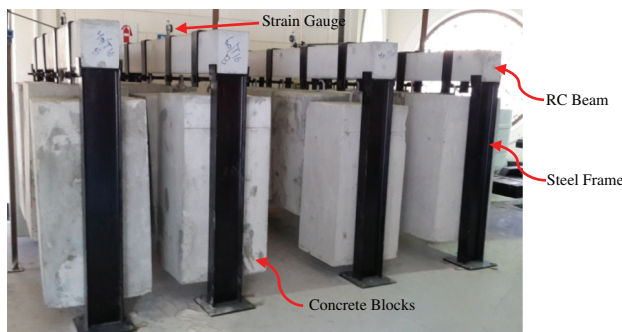


**Fig. 6.** Long term deflection test set up.

**Table IV.** Compressive and splitting tensile strength test results.

Mix code	Average compressive strength $f'_c$ , MPa	Average splitting tensile strength $f_{ct}$ , MPa	Splitting tensile computed according strength $f_{ct}$ , to ACI-318 code, MPa
SCC40/0.35	57.33	3.768	4.320
SCC40/0.45	42.68	3.018	3.720
SCC50/0.35	64.74	4.158	4.590
SCC50/0.45	45.29	3.308	3.840
SCC60/0.35	65.46	4.298	4.610
SCC60/0.45	46.2	3.278	3.880

suggests that the original general model of the ACI-318 code<sup>1</sup> used for design purposes to calculate the shear strength (Eq. (10)) may be conservative in predicting the shear capacity of SCC. This may be attributed to the fact that the general ACI-318 code<sup>1</sup> equation for calculating the shear capacity (ACI-318 code equation 22.5.5.1) does not consider the effect of shear span to depth ratios in predicting the shear strength of concrete beams. Hence, wider range of shear span to depth ratios need to be considered in order to propose a modification to the general ACI-318 code<sup>1</sup> equation (ACI-318 code equation 22.5.5.1) that is applicable for all values of shear span to depth ratios.

#### 4.4. Long Term Deflection Test

Table VII summarizes the failure loads of the beams that were tested using four points loading scheme. It also summarizes the deflection readings taken immediately after hanging the concrete blocks on the beams as well as the deflection readings after 7 and 14 days and after 1 month, 2 months, 3 months, and 6 months.

First, the deflection readings taken immediately after hanging the concrete blocks can be compared to the

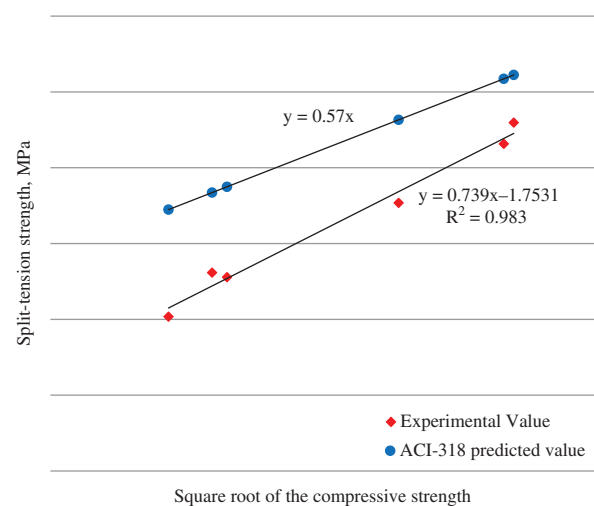


**Fig. 7.** Splitting tensile strength versus square root of compressive strength.

**Table V.** Compressive and modulus of rupture results.

Mix code	Average compressive strength $f'_c$ , MPa	Average modulus of rupture $f_r$ , MPa	Modulus of rupture $f_r$ , computed using ACI-318 code equation, MPa
SCC40/0.35	53.61	5.66	4.54
SCC40/0.45	41.93	4.14	4.01
SCC50/0.35	46.93	5.07	4.25
SCC50/0.45	42.51	4.17	4.04
SCC60/0.35	51.61	5.72	4.45
SCC60/0.45	37.94	4.08	3.82

instantaneous deflections computed using the following equation:

$$\Delta_i = \frac{5wL^4}{384E_cI_e} \quad (\text{For simply supported beams}) \quad (11)$$

Where,  $\Delta_i$  = immediate deflection, mm;  $w$  = total uniformly distributed load on the beam, kN/m;  $L$  = span length between supports, mm;  $E_c$  = concrete modulus of elasticity, MPa; and  $I_e$  is the section effective moment of inertia (assumed equal to the gross moment of inertia for immediate deflection calculations), mm<sup>4</sup>.

*Example: Mix SCC40/0.45:*

The total uniformly distributed load on the beam is computed as follows.

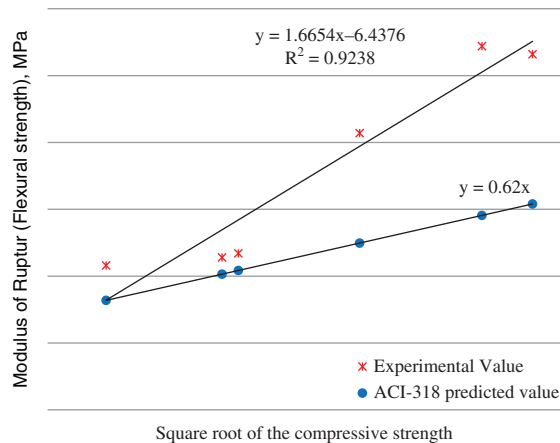
$w$  = self-weight of concrete beam + superimposed blocks weight considered as uniform load. Assuming density of reinforced concrete  $\gamma_c = 25$  kN/m<sup>3</sup>,

$$w = (A_{\text{Section}} \times \gamma_c) + \left( \frac{W_{\text{block}}}{d_{\text{between blocks}}} \right) \quad (12)$$

$$w = (0.2 \times 0.25 \times 25) + \left( \frac{10}{0.45} \right) = 23.47 \text{ kN/m}$$

$$E_c = 4700\sqrt{f'_c} \quad (\text{as per ACI-318, Section 19.2.2}) \quad (13)$$

$$E_c = 4700\sqrt{42.2} = 30531.9 \text{ MPa}$$

**Fig. 8.** Modulus of rupture versus square root of compressive strength.**Table VI.** Shear strength test results.

Mix code	Average compressive strength $f'_c$ , MPa	Experimental average shear stress $v$ , MPa		Shear stress $v$ , according to ACI equation, MPa
		Shear span/depth $\approx 1.5$	Shear span/depth $\approx 2.0$	
SCC40/0.35	56.09	4.29	3.11	1.25
SCC40/0.45	46.83	4.93	2.51	1.44
SCC50/0.35	60.54	5.60	2.48	1.30
SCC50/0.45	38.31	4.55	2.21	1.03
SCC60/0.35	54.68	4.16	2.83	1.23
SCC60/0.45	39.48	3.47	2.27	1.05

$$I_e = I_g = \frac{bh^3}{12} \quad (\text{for rectangular section}) \quad (14)$$

$$I_e = \frac{200 \times 250^3}{12} = 260.417 \times 10^6 \text{ mm}^4$$

$$\Delta_i = \frac{5 \times 23.47 \times 2250^4}{384 \times 30531.9 \times 260.417 \times 10^6} = 0.985 \text{ mm}$$

Similarly, the immediate deflection for mix SCC60/0.35 was found to be equal to 0.861 mm.

It is worth noting that the experimental immediate deflection values are in good agreement with those computed manually assuming un-cracked section.

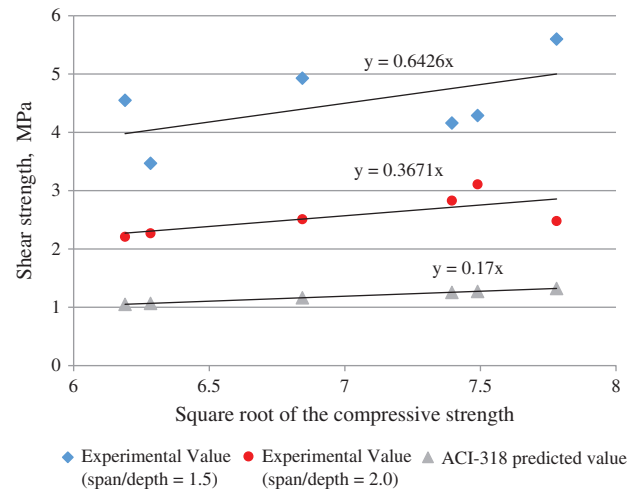
Long-term deflection resulting from creep and shrinkage of flexural members (normal weight or lightweight concrete) shall be determined by multiplying the short deflection, caused by sustained load, by the following factor (ACI-318, Section 9.5.2.5<sup>1</sup>):

$$\lambda_{\Delta} = \frac{\xi}{1 + 50\rho'} \quad (15)$$

Where  $\rho'$  = compression reinforcement ratio at mid span for simple and continuous spans, and at support for cantilevers; and  $\xi$  = time-dependent factor for sustained loads equal to the following:

60 months or more...2.0

12 months...1.4

**Fig. 9.** Shear strength versus square root of compressive strength.



**Table VII.** Long term deflection test results.

Mix code	Average compressive strength $f'_c$ , MPa	Beam ID	Failure load, kN	Deflection readings, mm						
				Immediate	7 days	14 days	1 month	2 months	3 month	6 months
SCC40/0.45	42.20	40T20	183.18	0.971	1.321	1.323	1.667	1.667	2.114	2.836
		40T16	163.7	1.100	1.704	1.811	1.989	2.184	2.496	3.101
SCC60/0.35	55.23	60T20	169.35	0.905	1.398	1.400	1.611	1.732	2.156	3.048
		60T16	167.07	1.057	1.709	1.822	2.010	2.154	2.244	3.414

6 months...1.2

3 months...1.0.

It should be noted that the short term deflection in this case is not equal to the immediate deflection. The short term deflection considers the cracked section. On the other hand, the immediate deflection uses the gross section to calculate the effective moment of inertia of the section because the maximum moment due to the sustained load at that stage (immediate),  $M_i$ , is less than the cracking moment. However,  $M_{cr}$  is computed using the following equation:

$$M_{cr} = \frac{f_r I_g}{y} \quad (\text{as per ACI-318, Section 19.2.3.1}) \quad (16)$$

Where,  $f_r$  = modulus of rupture, MPa,  $I_g$  = gross moment of inertia of the section,  $\text{mm}^4$ ; and  $y$  = half of section depth; mm.

The modulus of rupture,  $f_r$ , is computed using the following equation:

$$f_r = 0.62 \sqrt{f'_c} \quad (\text{as per ACI-318, Section 24.2.3.5}) \quad (17)$$

$$f_r = 0.62 \times \sqrt{42.2} = 4.03 \text{ MPa}$$

$$M_{cr} = \frac{4.03 \times 260.417 \times 10^6}{125} \times 10^{-6} = 8.4 \text{ kN} \cdot \text{m}$$

The maximum bending moment,  $M_i$ , is computed the following equation:

$$M_i = (A_{\text{Section}} \times \gamma_c) \frac{L^2}{8} \quad (18)$$

$$M_i = (0.2 \times 0.25 \times 25) \times \frac{2.25^2}{8} = 0.79 \text{ kN} \cdot \text{m} < M_{cr}$$

However, the effect of the hanged blocks took place after this immediate behavior. This allows the maximum

moment  $M_a$  to exceed the cracking moment as shown in the following equation:

$$M_a = w(\text{calculated in Eq. (12)}) \times \frac{L^2}{8} \quad (19)$$

$$M_a = 23.47 \times \frac{2.25^2}{8} = 14.85 \text{ kN} \cdot \text{m} > M_{cr}$$

→ cracked section

Hence, to compare the experimental long term deflections with those computed using ACI-318<sup>1</sup> approach, the short term deflection should be first calculated considering the cracked section moment of inertia. Details for calculating effective moment of inertia for deflection calculations can be found in ACI-318 Section 24.2.3.5.<sup>1</sup> Table VIII summarizes the effective moment of inertia computed as per ACI-318 code,<sup>1</sup> short term deflections, experimental deflection readings after 3 months and 6 months, and long term deflections computed using ACI-318 code.<sup>1</sup>

Table VIII shows that the experimental deflection readings at 3 months were less than or approximately equal to the values computed using ACI-318 code.<sup>1</sup> However, ACI-318 code<sup>1</sup> formula was found to underestimate the 6 month deflections of SCC beams. This indicates that the long term deflection of SCC beams is higher than that of NVC. The difference between the long term deflection of SCC and NVC elements may increase with time as the creep and shrinkage effects become more significant with time. This agrees with the findings of Mazzotti and Savoia<sup>24</sup> who reported that the total shrinkage and creep deflections of SCC beams is more than those of NVC. Hence, using the ACI-318 code<sup>1</sup> equation for the deflection of NVC elements may underestimate the actual long

**Table VIII.** Comparison between experimental deflections and long term deflections computed using ACI-318 code after 3 months and 6 months.

Mix code	Beam ID	Effective moment of inertia, $I_e$ , $\times 10^6 \text{ mm}^4$	Short term deflection, mm	Experimental long term deflection readings, mm		Long term deflections computed according to ACI-318 code, mm	
				3 month	6 months	3 month	6 months
SCC40/0.45	40T20	156.42	1.640	2.114	2.836	2.606	2.799
	40T16	154.04	1.665	2.496	3.101	2.645	2.842
SCC60/0.35	60T20	159.89	1.402	2.156	3.048	2.228	2.393
	60T16	158.31	1.416	2.244	3.414	2.250	2.417

term deflection of SCC beams. Hence, more research work should be directed towards this end.

## 5. CONCLUSIONS

The mechanical properties of the SCC and NVC elements can be different. In this paper, the experimental results of splitting tensile strength, modulus of rupture, shear strength and long term deflection of SCC elements were compared with those obtained using ACI-318 code<sup>1</sup> equations that were originally developed for NVC. In light of this study, the following conclusions can be drawn:

- The splitting tensile strength of SCC was found equal to 0.878 that of NVC. A trial was made to propose a formula to compute the splitting tensile strength of SCC however; more experimental data is required to validate this formula.
- The ACI-318 code<sup>1</sup> equation related to the modulus of rupture used for NVC was found to be conservative for SCC. A trial was made to propose a formula to predict the same of SCC however; more experimental data is required to validate this formula.
- The shear strength of the SCC was found to be dependent on the shear span to depth ratio similar to the behavior of NVC. However, the shear strengths computed using the ACI-318<sup>1</sup> formula were found to be conservative for all shear span to depth ratios investigated in this study. Hence, further tests are needed to investigate beams with wider range of shear span to depth ratios in order to propose a formula to predict the shear behavior of SCC and to be applicable to all shear span to depth ratios.
- The experimental deflection readings at 3 months are a less than or approximately equal to the values computed using ACI-318 code<sup>1</sup> formula. However, ACI-318 code<sup>1</sup> formula was found to underestimate the long term deflections of SCC beams at 6 months.
- The long term deflection of SCC beams is more than that of NVC and the difference between the long term deflection of SCC and NVC elements may increase with time as the creep and shrinkage effects become more significant with time.
- ACI-318 code<sup>1</sup> formulas for calculating the deflection of NVC elements may underestimate long term deflection of SCC elements. Hence, more research effort should be directed towards this end.

**Acknowledgment:** This report was made possible by a National Priority Research Program award [NPRP 6-280-2-117] from the Qatar National Research Fund (a member of The Qatar Foundation). The statements made herein are solely the responsibility of the authors. The technical support of ALWATANIYA ready mix company at Qatar in the development of this work is gratefully acknowledged.

## References and Notes

1. ACI Committee 318, Building Code Requirements for Structural Concrete (ACI 318M-14) and Commentary (318RM-14), American Concrete Institute, Farmington Hills, MI (2014), p. 519.
2. K. Tanaka, K. Sato, S. Watanabe, I. Arima, and K. Suenaga, *ACI Special Publication* 140, 25 (1993).
3. T. Fukute, A. Moriwake, K. Sano, and K. Hamasaki, *ACI Special Publication* 154, 335 (1995).
4. M. Hayakawa, Y. Matsuoka, and K. Yokota, *ACI Special Publication* 154, 381 (1995).
5. H. Kitamura, K. Ukaji, and H. Okamura, *Concrete for Infrastructure and Utilities* 1996, 469 (1996).
6. M. Ouchi, *Proceedings of the Second International Symposium on Self-Compacting Concrete* (2001).
7. K. H. Khayat and R. Morin, *3rd International RILEM Symposium on Self-Compacting Concrete* (2003).
8. S. Z. Yuce, E. Yuksel, Y. Bingol, K. Taskin, and H. F. Karadogan, *Structural Engineering and Mechanics* 27, 589 (2007).
9. T. Albanesi, D. Lavorato, C. Nuti, and S. Santini, *European Journal of Environmental and Civil Engineering* 13, 671 (2009).
10. C. E. Chalioris and C. N. Pourzitidis, *ISRN Civil Engineering* 2012 (2012).
11. C. E. Chalioris, C. P. Papadopoulos, C. N. Pourzitidis, D. Fotis, and K. K. Sideris, *Journal of Engineering* 2013, Article ID 912983 (2013), 12 pages.
12. C. E. Chalioris, G. E. Thermou, and S. J. Pantazopoulou, *Construction and Building Materials* 55, 257 (2014).
13. Rakesh Kumar, *Journal of Civil and Environmental Engineering* 5, 176 (2015).
14. M. Mallesh, G. C. Shwetha, K. Reena, and Madhukaran, *International Journal of Science, Engineering and Technology Research (IJSETR)* 4, 3237 (2015).
15. O. S. Olafusi, A. P. Adewuyi, A. I. Otunla, and A. O. Babalola, *Open Journal of Civil Engineering* 5, 1 (2015).
16. K. Holschemacher and Y. Klug, *LACER* 7, 123 (2002).
17. P. L. Domone, *Cement and Concrete Composites* 29, 1 (2007).
18. B. Craeye, P. Van Itterbeeck, P. Desnerck, V. Boel, and G. De Schutter, *Cement and Concrete Composites* 54, 53 (2014).
19. Emadaldin Mohammadi Golafrshani and Ashraf Ashour, *Automation in Construction* 64, 7 (2016).
20. C. Parra, M. Valcuende, and F. Gómez, *Construction and Building Materials* 25, 201 (2011).
21. F. M. A. Filho, B. E. Barragán, J. R. Casas, and A. L. H. C. El Debs, *Construction and Building Materials* 24, 1608 (2010).
22. Y. H. Kim, M. B. D. Hueste, D. Trejo, and D. B. H. Cline, *Journal of Structural Engineering* 136, 989 (2010).
23. V. Boel, P. Helincks, P. Desnerck, and G. De-Schutter, *Bond Behaviour and Shear Capacity of Self-Compacting Concrete*, Springer, Netherlands (2010).
24. C. Mazzotti and M. Savoia, *ACI Structural Journal* 106, 772 (2009).
25. ACI Committee 237, Self-Consolidating Concrete (ACI 237R-07), American Concrete Institute, Farmington Hills, MI (2007), p. 30.
26. ASTM C192/C192M-16a, Standard Practice for Making and Curing Concrete Test Specimens in the Laboratory, ASTM International, West Conshohocken, PA (2016), p. 8.
27. R. H. Harkouss and Bilal Salim Hamad, *International Journal of Concrete Structures and Materials* 9, 69 (2015).
28. ASTM C1064/C1064M-12, Standard Test Method for Temperature of Freshly Mixed Hydraulic-Cement Concrete, ASTM International, West Conshohocken, PA (2012), p. 3.
29. BS EN 12350-8, Testing Fresh Concrete: Self-Compacting Concrete—Slump-Flow Test, BSI, UK (2010), p. 14.
30. BS EN 12350-9, Testing Fresh Concrete: Self-Compacting Concrete—V-Funnel Test, BSI, UK (2010), p. 12.
31. The European Guidelines for Self-Compacting Concrete: Specification, Production and Use, EFNARC (2005), Vol. i–v, p. 63.

32. ASTM C470/C470M-15, Standard Specification for Molds for Forming Concrete Test Cylinders Vertically, ASTM International, West Conshohocken, PA (2015), p. 5.
33. ASTM C39/C39M-16, Standard Test Method for Compressive Strength of Cylindrical Concrete Specimens, ASTM International, West Conshohocken, PA (2016), p. 7.
34. ASTM C496/C496M-11, Standard Test Method for Splitting Tensile Strength of Cylindrical Concrete Specimens, ASTM International, West Conshohocken, PA (2011), p. 5.
35. ASTM C78/C78M-15b, Standard Test Method for Flexural Strength of Concrete (Using Simple Beam with Third-Point Loading), ASTM International, West Conshohocken, PA (2016), p. 4.
36. ASTM A615/A615M-16, Standard Specification for Deformed and Plain Carbon-Steel Bars for Concrete Reinforcement, ASTM International, West Conshohocken, PA (2016), p. 8.
37. ASTM E178-08, Standard Practice for Dealing with Outlying Observations, ASTM International, West Conshohocken, PA (2008), p. 18.
38. G. N. J. Kani, *Journal of the American Concrete Institute* 61, 441 (1964).